This is a peer-reviewed, accepted author manuscript of the following research article: Zaman, T, Feng, Z, Mitra, S, Syed, M, Karanki, S, Villa, L & Burt, G 2023, 'ANN driven FOSMC based adaptive droop control for enhanced DC microgrid resilience', IEEE Transactions on Industry Applications. https://doi.org/10.1109/TIA.2023.3328577

ANN Driven FOSMC Based Adaptive Droop Control for Enhanced DC Microgrid Resilience

Taimur Zaman, Zhiwang Feng, Sanjib Mitra, *Student Member, IEEE,* Mazheruddin Syed, *Member, IEEE,* Srinivas Karanki, *Senior Member, IEEE,* Luiz Villa and Graeme Burt, *Member, IEEE*

***Abstract*—Parallel operation of power converters in islanded DC microgrids exhibits significant trade-off in voltage regulation and current sharing with conventional droop control. The converters exhibit inaccuracies in proportionate sharing of current when subject to heavy and transient loading while sharing a common bus. Moreover, the inaccuracies further persist due to unmodeled dynamics, parametric uncertainties, disturbance in the system and communication reliability. Therefore, the resilient parallel operation of power converters in DC microgrids requires a robust and fast control strategy that can mitigate the effect of disturbances and maintain regulated bus voltage with proportional current sharing amongst the power converters. Consequently, this work proposes a novel ANN driven droop control for a DC microgrid to enhance the transient response and mitigate disturbance in finite time. Two controllers based on adaptive droop strategy are proposed; the primary controller is a generalized Hebb's learning law-based PI integrated controller that can adjust the gains in real time for finite-time disturbance compensation in the networks and the secondary control regulates the bus voltage using fractional order sliding mode control. The effectiveness of the proposed method is evaluated by simulation and experiment and compared with the conventional and distributed droop control methods, proving its robust and adaptive performance for resilient DC microgrid applications.**

***Index Terms*—DC-DC converter, artificial neural networks, DC microgrid, sliding mode control.**

I. Introduction

THE global concern to mitigate carbon emissions and preserve the environment from further depletion presents a challenge for which the scientific community is actively developing alternate and efficient methods to harvest energy from Renewable Energy Sources (RES). Since RES are highly intermittent in nature, a challenge in terms of their integration within existing system for stable power flow exists. To address this challenge and to improve the resilience of the power system, microgrids were first introduced to facilitate the integration of intermittent RES to a common point [1].

Amongst different variants of microgrids, DC microgrids are simple, reliable and possess natural DC coupling for RES, rendering the integration and control more convenient and advantageous as compared to other variants of microgrids [2]. However, the operational resilience of such networks is highly dependent upon their operation under unmodelled system dynamics, disturbances, and outages of DERs. To address the challenges with the operational resilience of such networks, different control methods based on distributed, centralized and decentralized approaches were proposed in the literature [3].

The widely adopted technique within DC networks is decentralized control, where a droop-based strategy holds a pivotal role in proportionate sharing of the load current and maintaining the desired bus voltage among interconnected converters [4]. The strategy solely hinges on the settings of the droop gains and can be implemented within the primary loop of the decentralized approach, thus ensuring equitable current sharing amongst the interconnected DGs [5]. However, the efficacy of proportionate current sharing declines notably when initial design parameters of the DC microgrid are varied [6], [7]. The changes in the line impedance linking the load bus and Power Converters (PCs) introduce challenges in intended current and voltage regulations. As a result, individual PCs are overloaded, subsequently leading to a deterioration in bus voltage regulation and in turn, pose a challenge to the operational resilience of the entire microgrid [8]. Therefore, to counteract the aforementioned drawbacks, it is common practice to implement supplementary control layers.

Supplementary control layers can be realised by centralized approach [9], however, they rely upon expensive communications network to ensure the exchange of essential information from the DGs and to dispatch of control commands to the DGs. Centralized control approaches are typically designed to handle substantial influx of data and subsequent processing and can therefore be more expensive. Furthermore, centralized approaches are vulnerable to single point of failure [10] significantly challenging resilience of the approach. As a consequence, distributed control methods are widely proposed where the DGs only communicate with their neighbors. Distributed control methods offer a viable alternative and address the challenges posed by the centralized approaches, alleviating the communication and computational burdens, while concurrently enhancing the scalability and resilience.

Fig. 1 shows the concept of a typical DC microgrid with RES integrated into the common bus using PCs that are connected in parallel and typically share the load bus current in proportion to the DG capacity. Conversely, the DGs in such a scheme are operated with droop control as primary and the aforementioned as secondary controller [11]. However, the effectiveness of the additional layers often hinges on the communication schemes, which can either be distributed or centralized. In this regard, the cumulative response of control layers and communication strategy reflects the collective performance that contributes to the system's resilience against transients and disturbances requiring finite time response of the controllers [12]. Therefore, to alleviate the computational burden and achieve faster and more dynamic responses in the distributed control approach, the dynamic consensus algorithm is considered a favorable approach [13]. The method is es-

sentially proposed to relieve the communication burden by averaging the microgrid voltage and regulating it to the desired set point [9]. Similarly, a virtual voltage-droop based approach was proposed to guarantee the bus voltage restoration and current sharing through a consensus algorithm in [14]. Likewise, an asymptotically rapid convergence speed characterized by an inexplicit convergence time was introduced in [15]. The method is further addressed by a fixed time-based consensus algorithm proposed in [16]. However, most of the consensus-based methods require an additional computational resource to optimize and obtain global gains for the droop settings [17]. Therefore, the proposed approaches are unsuitable for DC microgrids requiring fast and dynamic response. Further, the approach suffers from communication delays and results in unregulated bus voltage and uneven current sharing [9].

In efforts to achieve fast and dynamic response using the conventional droop method as the primary control, the authors in [18] proposed an adaptive droop method to regulate the bus voltage and to maintain the State of Charge (SoC) of batteries in a decentralized system. Apart from this, several approaches based on the nonlinear droop gains adjustment concept were proposed in [19]–[22]. The methods demonstrate proportionate current sharing and bus voltage regulation. However, it is unrealistic to consider the constant parameters of the system for real-time applications. In addition, the proposed approaches do not guarantee the stability of the network and lack integration with distributed approaches for compensating uncertain conditions of the network.

Further, the dynamic loading conditions demand asymptotically stable control with fast dynamics to ensure the resiliency of the system against disturbances in the network. Most of the methods report droop control with distributed approach or linearization techniques, which result in tracking inaccuracies [23]–[26]. The time-varying disturbance and parameter uncertainties result in inevitable deviations in current sharing and bus voltage due to the invariant droop coefficients. Some of the well-known methods, such as fuzzy logic, model predictive, H_∞, sliding mode control (SMC) and Neural Networks (NN), were proposed to enhance the stability and performance of the system. The SMC was reported in a hybrid format with conventional droop control for parallel connected buck converters in DC microgrid [24]. Similarly, the authors proposed a PI controller to adjust the droop gains to reduce the current error, however, the method lacks information regarding stability during mismatched dynamic disturbances. Similarly, the authors in [25] proposed sub-optimal second-order SMC using a droop technique to illustrate the performance of controllers for equal power sharing only and did not consider disturbance mitigation. Consequently, nonsingular terminal SMC [27] and integer order SMC [28] were proposed to compensate for time-varying disturbances in stand-alone DC-DC converter systems. However, the method remains void for the dynamic mismatched disturbances. In this context, the generalized fractional order control provides more degrees of freedom for achieving the optimum dynamic response. The authors in [29] proposed the SMC with fractional order theory to enhance the reference tracking with finite time disturbance compensation for buck converters. Similarly, the adaptive fractional order

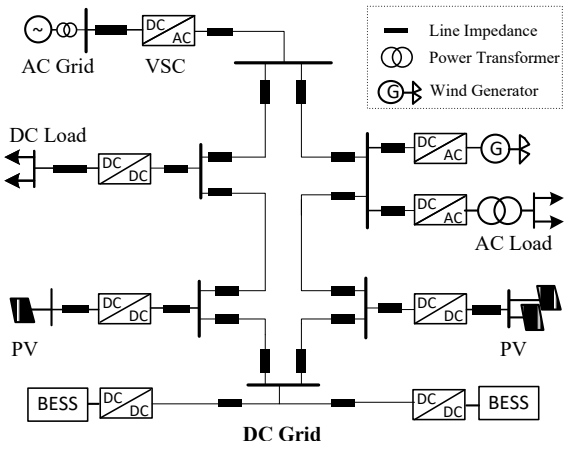

Fig. 1: A representation of DC Microgrid.

sliding mode control (FOSMC) was proposed in [30] for mismatched disturbances in the system and the performance was evaluated for real-time disturbance mitigation. Though the method mitigates the disturbance successfully, it does not comply with the droop control strategy for proportionate current sharing.

The authors in [31] suggested an adaptive PI controller whose gains are adjusted online for real-time disturbance mitigation in DC/DC converters. The approach is more efficient with fast dynamics for finite time disturbance compensation, however, the performance is not evaluated in cascaded feedback control. The application of this approach in conjunction with integer order SMC is more rare for buck/boost converters using droop control to ensure the proportionate current sharing while mitigating disturbances in finite time [26]. Motivated by addressing the limitations of the aforementioned methods in the literature, this work proposes a novel adaptive droop control strategy for DC microgrid to enhance its operational resiliency. The main contributions are summarized as follows:

1) A novel Artificial Neural Networks (ANN) driven FOSMC-based adaptive droop controller is proposed to ensure equal current sharing and balanced bus voltage of parallel connected converters in DC microgrids.
2) A Generalized Hebb Learning (GHL) based single layer feedforward adaptive controller is proposed to adjust online droop gains during parametric uncertainty and disturbance in the system to ensure enhanced operational resiliency of the system.
3) The effectiveness of the proposed method is evaluated under varied loading conditions, parametric uncertainty, mismatched impedances, delays and loss of DGs. The performance of the method is further compared with state-of-the-art methods in literature and validated by real-time hardware prototyping.

The rest of the paper is organized as follows: Section II discusses the conventional droop method and its limitations, while Section III presents the preliminary modeling of power converters, controller formulation, and problem identification. The numerical results with experimental validation are pro-

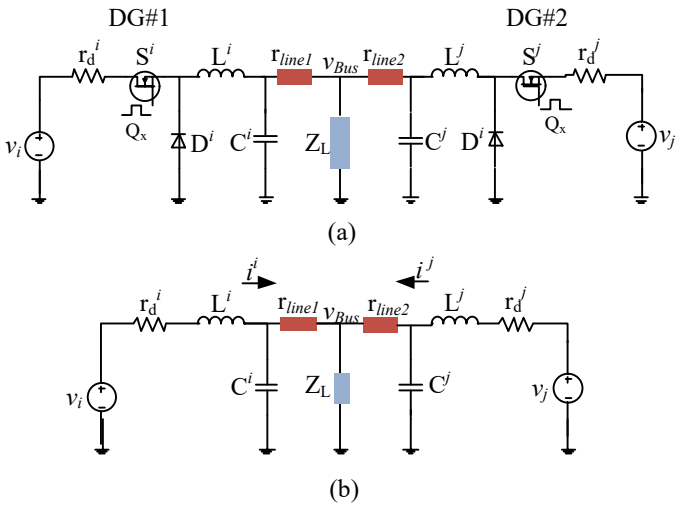

Fig. 2: Equivalent circuit of parallel connected converters in DC microgrid: (a) parallel connection of buck converters circuit, (b) operating condition for PWM $\rightarrow high$.

vided in Section IV. Section V concludes the paper.

II. Droop Control of DC Microgrid

The conventional droop control technique enables the proportionate sharing of load power on the main bus while connecting PCs in parallel. The output voltage of parallel connected PCs is computed by constant droop coefficients. This generates a virtual reference for each converter which is compared to the actual bus voltage. The difference in these values triggers the internal control loop of each converter to generate the proportionate current.

Fig. 2 refers to a simplified circuit of two parallel connected DGs in a DC microgrid feeding a common and Constant Power Load (CPL). The two DGs are connected through lines of different lengths with unequal resistance and denoted by r_{line1} and r_{line2} for DG_i and DG_j respectively. Z_L refers to the impedance of the common load connected across the parallel connected DGs. The terminal voltage and droop resistance for both DGs are denoted by v^i, v^j and r_d^i, r_d^j respectively. The equation for the voltage reference of each converter can be written as,

$$\begin{bmatrix} v^i \\ v^j \end{bmatrix} = v_{bus} + \begin{bmatrix} r_d^i & 0 \\ 0 & r_d^j \end{bmatrix} \begin{bmatrix} i_{max}^i \\ i_{max}^j \end{bmatrix} \tag{1}$$

where v_{bus} refers to the main bus voltage and $\begin{bmatrix} i_{max}^i \, i_{max}^j \end{bmatrix}^{\mathbf{T}}$ is the maximum output current of each converter. Considering the maximum allowable deviation in terminal voltage of each converter, the droop coefficients can be computed as,

$$r_d^{i,j} = \frac{\Delta v_{max}^{i,j}}{i_{max}^{i,j}} \tag{2}$$

where, $\Delta v_{max}^{i,j}$, $i_{max}^{i,j}$ refers to the maximum allowable voltage and current deviations in each PC. These constant coefficients depend on PC dynamics and control constraints to vary system parameters (voltage and current) for any dynamic load and disturbance in the system as shown in Fig. 3(a,b). For instance, low droop gains result in tight voltage regulation for loading conditions and disturbances, however, results in a

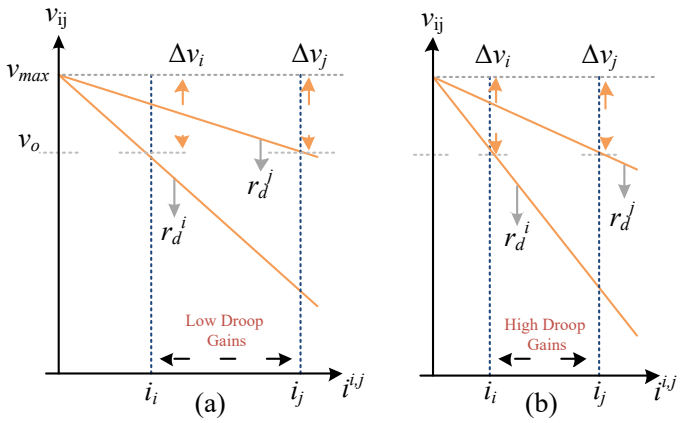

Fig. 3: Voltage and current variation of converters using linear droop curves for (a) low droop gains, (b) high droop gains.

definite mismatch of proportionate current sharing. The case is opposite for higher droop gains and this can be mathematically interpreted as

$$r_d^{i,j} \leq \Delta v_{max}^{i,j} \frac{v^{i,j}}{P^{i,j}} \tag{3}$$

where $P^{i,j}$, and $v^{i,j}$, refers to the rated power and voltage of power converters associated with $DG^{i,j}$ [32].

Moreover, apart from the impedance constituted due to converter dynamics, the total impedance seen by each DG from its terminals to the load point can be written as

$$Z^i = \underbrace{r_d^i + r_{line1}}_{r_{droop}^i} + Z_L, \quad Z^j = \underbrace{r_d^j + r_{line2}}_{r_{droop}^j} + Z_L \tag{4}$$

It is impractical to consider the line resistance of each converter to be equal to each other. Therefore, the difference in the current resulting from the mismatched impedances can be computed by applying Kirchhoff's law to the parallel connected converters as shown in Fig. 2(b). This yields

$$\begin{aligned} i^i - i^j = \; & 2\left(v^i - v^j\right)\left[\frac{1}{Z^i + Z^j + \frac{Z^i \cdot Z^j}{Z_L}}\right] + \ldots \\ & \left[v^i \cdot Z^j - v^j \cdot Z^i\right]\left[\frac{1}{Z^i \cdot Z^j + Z^i \cdot Z_L + Z^j \cdot Z_L}\right] \end{aligned} \tag{5}$$

From (1) - (5), it is evident, that the proportionate current sharing strategy in traditional droop control purely relies on the loading current and droop coefficients of each converter in parallel connected DGs. Furthermore, the variation in overall impedance and line resistance impacts the proportionate current-sharing accuracy. The larger droop gains results in less current deviation of the parallel connected converters, however considerably increase the voltage deviations resulting in voltage fluctuations of the common bus voltage [8].

Fig. 4 illustrates the performance of the conventional droop method applied to parallel connected converters under the variations in line impedance. The converters provide proportionate power to the load as long as the overall impedance remains the same. However, 5% variation in one converter impedance significantly deteriorates the equal current sharing strategy. This trade-off in the current and voltage is the manifestation of smaller droop gains chosen through the linear droop method which results in unequal current sharing. The issue can be

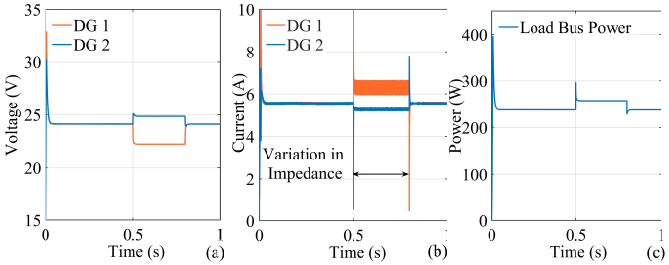

Fig. 4: Effect of variation in line impedance of parallel connected converters on (a) voltage, (b) current, (c) load bus power.

resolved by adopting droop gains using the nonlinear method as briefly discussed in [21]. This can be achieved by adjusting the current reference of each converter in a finite time as soon as the deviation in the reference voltage increases. For the sake of simplicity, using (2), (4) and considering $i_{max}^{i,j} = I_{ref}^{i,j}$, (1) can be rewritten as,

$$I_{ref}^{i,j} = \frac{1}{r_d^{i,j}} \left[v_{bus} - v^{i,j} \right] \tag{6}$$

For the PC interfaced sources $(i \cdots j)$, (6) can be manipulated for the reference current as,

$$r_d^i \dot{I}_{ref} = v_{bus} - v^i - r_d^j \cdot i^j \tag{7}$$

$$I_{ref} = \frac{\left[v_{bus} - v^{i,j} \right]}{r_d^{i,j}} - \frac{r_d^i}{r_d^j} \cdot i^j \tag{8}$$

This provides the final expression for the droop gains which can be adjusted in finite boundary limits for all loading conditions of the converters associated with DGs connected in parallel to the common bus [21]. The adjustment of droop gains requires a fast and dynamic method that precisely defines the setpoint for the secondary controller to regulate the output voltage and current of each converter and provide stabilized load current and voltage across the common bus.

III. Proposed Hybrid Adaptive Droop Controller

The issue of disproportionate current sharing and unregulated bus voltage in the DC microgrid has been established in Section I. To address this challenge of ensuring proportionate current sharing while regulating the bus voltage of the DC microgrid, a two-level control is proposed. The two-level control comprises a primary and a secondary control. The secondary control loop uses a fractional order SMC to establish a constant bus voltage. The reference for the secondary control is established by the primary loop, associated with the converter's output current and droop coefficients. To sustain a stable setpoint for secondary control to track the trajectories of reference voltage in the presence of transients, different loading and lumped disturbance, an adaptive PI controller is proposed. The adaptive control aims to eliminate the disturbance by adjusting the gains using GHL rule. Fig. 5 shows the block diagram of the proposed control mechanism for parallel connected PCs in a DC microgrid.

In efforts to address the challenge associated with the parallel operation of converters in DC microgrid for proportionate power sharing, the two controllers, primary and secondary, are

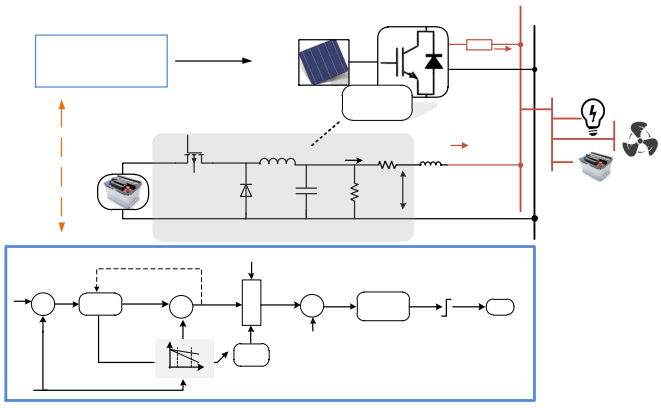

Fig. 5: Block diagram of proposed control system.

derived based on the state-space model of a buck converter operating in continuous conduction mode [9].

A. Controller Formulation

1) FOSMC Derivation: The basic topology of Buck converter having input voltage v_{in}^j, filtering inductor L^j and capacitor C^j with a cumulative output impedance Z^j is shown in Fig. 5. The dynamic model for voltage and output current can be written as

$$\begin{aligned} \dot{v}_o^j &= \frac{i_L^j}{C^j} - \frac{v_o^j}{Z^j C^j} + D_v, \\ \dot{i}_L^j &= -\frac{v_o^j}{L^j} + \frac{v_{in}}{L^j} u, \end{aligned} \tag{9}$$

where i_L^j and C^j refers to inductor current and filtering capacitor of converter j, respectively. The term Z^j refers to the lumped disturbance associated with impedance variations as shown in (4). The parametric uncertainty can be defined as $D_v = \delta \dot{v} + d_v(t)$. This refers to the variations in the dynamics of states with known upper boundary limits. The control signal for PWM generation is denoted by u. The voltage error can be written as

$$e_v^j = v_{ref}^j - v_o^j \tag{10}$$

where, v_{ref}^j refers to the reference voltage of the j^{th} converter. The time derivative of (10) can be written as

$$\dot{e}_v^j = \dot{v}_{ref}^j - \dot{v}_o^j \tag{11}$$

Using (9), (11) can be rewritten as

$$\dot{e}_v^j = \dot{v}_{ref}^j - \left[\frac{i_L^j}{C^j} - \frac{v_o^j}{Z^j C^j} + D_v \right] \tag{12}$$

where $Z^j = R^j + d^j$ is the nominal value of the resistance and lumped disturbance of the j^{th} converter. Taking the second derivative of (11), we get

$$\ddot{e}_v^j = \ddot{v}_{ref}^j - \frac{\dot{i}_L^j}{C^j} + \frac{\dot{v}_o^j}{Z^j C^j} - D_v \tag{13}$$

Substituting (9) in (13), we get

$$\ddot{e}_v^j = \ddot{v}_{ref,j}^j - \frac{1}{C_j} \left[-\frac{v_{o,j}}{L_j} + \frac{v_{in}}{L_j} u \right] + \frac{\dot{v}_{o,j}}{Z_j C_j} - D_v \tag{14}$$

For the sliding surface to be constructed, the lemma of fractional calculus is essential for deriving the switching control law and the surface convergence proof. Therefore, the definitions of fractional calculus and Lemma are presented next.

*2) **Preliminaries**:* The fractional operators are the suborders of traditional differential and integral order calculus. The differential operator can be defined as [22]

$$ {}_{t_0}D_t^{\mu} f(t) = \begin{cases} \frac{\mathrm{d}^{\mu}}{\mathrm{d}t^{\mu}} f(t), & \mu > 0 \\ f(t), & \mu = 0 \\ \int f(\tau)\mathrm{d}\tau^{-\mu}, & \mu < 0 \end{cases} \tag{15} $$

Definition 1: The Caputo-based definition of derivative function in fractional calculus is more frequent with its application to control engineering, and therefore based on [22], this work considers its definition as:

$$ {}_{t_0}^{C}D_t^{\alpha} y(t) = \frac{1}{\Gamma(m-\alpha)} \int_{t_0}^{t} \frac{y^{(m)}(\tau)}{(t-\tau)^{1+\alpha-m}} \mathrm{d}\tau, \tag{16} $$

where $\alpha \in \mathbb{R}$ & $m \in \mathbb{Z}$ such that for any $\mathbb{Z}$ the value of α must be greater than m.

Definition 2: The integral terms from the fractional calculus with order α can be written as,

$$ {}_{t_0}D_t^{-\alpha} G(t) = \frac{1}{\xi(\alpha)} \int_{t_0}^{t} \frac{G(\tau)}{(t-\tau)^{1-\alpha}} \mathrm{d}\tau, \tag{17} $$

Lemma 1: From Definition **1**, C can be denoted as subset of $\mathbb{R}(x)$: the bounded conditions holds for the fractional integrator $D_{x+}^{-\upsilon}$ and $D_{y-}^{-\upsilon}$ so that if $\mathbb{R}(C) > 0$, the conditions implies as,

$$ \begin{aligned} \|D_{x+}^{-\upsilon} g(x)\|_{\kappa} \leq & \Lambda \|g(x)\|_{\kappa}, \quad \|D_{y-}^{-\upsilon} g(x)\|_{\kappa} \leq \Lambda \|g(x)\|_{\kappa}, \\ \Lambda = & \frac{(y-x)^{R(c)}}{R(c)|\Gamma(c)|}. \end{aligned} \tag{18} $$

From the preliminary definition of fractional calculus and equation (15) and (17), the sliding surface for the converter can be written as

$$ s = c_1 D^{-\alpha} e_v^j + c_2 D^{\alpha} \left| e_v^j \right|^{\gamma} \tag{19} $$

Then the derivative of the sliding surface can be written as

$$ \dot{s} = c_1 D^{1-\alpha} \dot{e}_v^j + c_2 \gamma D^{\alpha} \left| e_v^j \right|^{\gamma-1} \ddot{e}_v^j \tag{20} $$

Using (14) and (20) can be simplified for the control law as,

$$ \begin{aligned} \dot{s} = & c_1 D^{1-\alpha} \left[\dot{v}_{ref}^j - \left[\frac{i_L^j}{C^j} - \frac{v^j o}{Z^j C^j} + D_v \right] \right] \\ & + c_2 \gamma D^{\alpha} \left| e_v^j \right|^{\gamma-1} \\ & \left[\ddot{v}_{ref}^j - \frac{1}{C^j} \left[-\frac{v_o^j}{L^j} + \frac{v_{in}}{L^j} u \right] - \frac{v_o^j}{Z^j} \right] \end{aligned} \tag{21} $$

Further simplifying for extracting the control equivalent control law (u=u_{eq}) by taking the $\dot{s} = 0$ gives

$$ \begin{aligned} u_{eq} = & -\frac{1}{v_{in}} \left| e_v^j \right|^{1-\gamma} \left[\frac{c_1}{c_2} D^{1-2\alpha} e_v^j - \frac{L^j}{v_o^j} - \right. \\ & \left. \frac{Z^j C^j}{v_o^j} + D_v \right] \end{aligned} \tag{22} $$

The overall control law can be defined as

$$ U_{fosmc} = u_{eq} + u_{disc} \tag{23} $$

where u_{disc} refers to the discontinuous component; however, to reduce the chattering, this part is replaced with $\tanh$ function to avoid switching stress. The control law defined in (23) can be written as

$$ \begin{aligned} U_{fosmc} = & -\frac{1}{V_{in}} \left| e_v^j \right|^{1-\gamma} \left(\frac{c_1}{c_2} D^{1-2\alpha} e_v^j - \frac{L^j}{v_o^j} - \ldots \right. \\ & \left. \frac{Z^j C^j}{v_o^j} + D_v \right) + \left| e_v^j \right|^{1-\gamma} \left[-\frac{\lambda}{\gamma c_2} \tanh\left(\frac{s}{\chi} \right) \right] \end{aligned} \tag{24} $$

To ensure the suitability of the controller for hardware implementation, the following assumptions are intrinsic to define.

***Assumption 1**:* The system states are measurable.

***Assumption 2**:* The system states have uncertainty & the parameters of states are known.

***Assumption 3**:* The control function u_{eq} is bounded $|||u_{eq}| \neq 0 \therefore 0 < |u_{eq}| \leq |u_{eq}^{max}|$

***Assumption 4**:* The external disturbances are unknown but with finite boundary limits $\implies \| D_v(t) = \delta v_o + d_v(t) \| \leq D_v^{max}$.

Theorem (A): Considering the assumptions for the states defined in (9), the control input derived in (24) will asymptotically converge the error to zero for the defined reference trajectory and any initial conditions.

Proof: This can be proven by choosing the Lyapunov candidate function as,

$$ V(S) = \frac{1}{2} S^2 \tag{25} $$

The first derivative of (25) gives

$$ \dot{V}(S) = S \underbrace{\left[c_1 D^{1-\alpha} \dot{e}_v^j + c_2 \gamma D^{\alpha} \left| e_v^j \right|^{\gamma-1} \ddot{e}_v^j \right]}_{\dot{S}} \tag{26} $$

Substituting (12) and (14) into (26), the equation can be expanded as (27).

Futhermore, the control input (u_{FOSMC}) from (24) can be used in (27) to obtain

$$ \dot{V}(S) = S \left\{ c_1 D^{1-\alpha} \left(\dot{v}_{ref}^j - \left[\frac{i_L^j}{C^j} - \frac{v_o^j}{Z^j C^j} + D_v \right] \right) + c_2 \gamma D^{\alpha} \left| e_v^j \right|^{\gamma-1} \left[\ddot{v}_{ref}^j - \frac{1}{C^j} \left[-\frac{v_o^j}{L^j} + \frac{v_{in}}{L^j} u \right] - \frac{v_o^j}{Z^j} \right] \right\} \tag{27} $$

$$\begin{aligned}\dot{V}(S) &= S\dot{S} \\ &= S\left[\frac{c_1}{c_2} - \frac{\lambda}{c_2}\tanh\left(\frac{S}{\chi}\right) + D_v(t)\right] \\ &= S\frac{c_1}{c_2} - S\frac{\lambda}{c_2}\tanh\left(\frac{S}{\chi}\right) + SD_v(t)\end{aligned} \tag{28}$$

where $\tanh(S)$ can be defined as

$$\tanh(S) = \begin{cases} 1, & \text{if } S \geq \epsilon \\ -1, & \text{if } S \leq \epsilon \end{cases} \tag{29}$$

ϵ is a small positive constant and thus referring to (28), where careful selection of coefficients for c_1, c_2, λ, and χ satisfy the conditions of Lyapunov function derivative converging to zero over time when the coefficients $[c_1, c_2, \lambda, \chi] \geq [D_v(t)^{max}]$.

B. Adaptive PI Control

The droop coefficient of each converter is directly related to its branch current as derived in equations (2) – (8). Since the droop-based strategy is applied at the primary level, any discrepancy in the load current results in deviated reference for the secondary controller as shown in Fig. 5. In efforts to mitigate the inaccuracy in reference generation for the secondary controller, the droop value must be compensated using an adaptive PI controller. Therefore, a novel adaptive PID with NN-based single-layer feed-forward GHL method is proposed as is illustrated in Fig. 6. It is a derived form of unsupervised learning, where the correlation between the desired output and input values is achieved by updating the weights of connection between the neurons. This weight adjustment occurs when interconnected neurons are triggered at the same value. The weights are initialized with an arbitrarily small value and change concurrently with variations in the state vector while following the GHL rule [26]. These variations in the state vector are the manifestation of parametric uncertainty, impedance variations, or communication failure, which trigger the activation function and the initial weights are updated accordingly. The final value of the weights is decided when the connection between neurons is strengthened and error is minimized by ensuring an optimum correlation between the reference and output values. The training data and learning relation are updated online at each time step of the corresponding input state vector.

The learning relation between the updated synaptic weights (**w**) and the corresponding input $x^{i,j}$ and output $y^{i,j}$ states can be written as

$$\mathbf{w}(k+1) = \mathbf{w}(k) + \eta y(k) x(k) \tag{30}$$

where η is the learning rate.

The weights in conventional Hebb learning law exhibit continuous growth during the learning process and do not converge to provide a solutions for the steady and transient state of the system thus asymptotic convergence of the controller cannot be guaranteed [33]. Therefore, the GHL rule is adapted to ensure a solution in both steady and transient states by assuring the statistical aspects of the input for

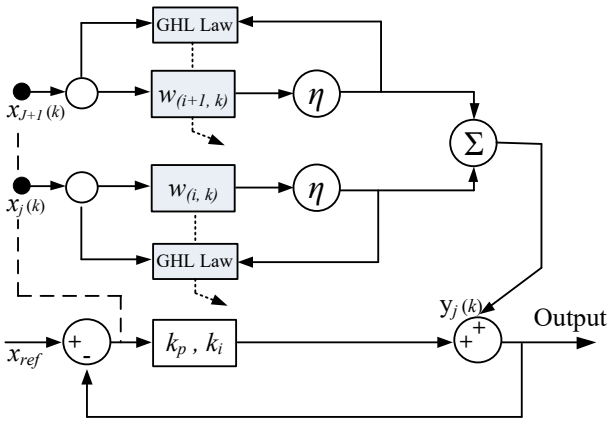

Fig. 6: Block diagram of GHL rule.

weight adjustments to provide accepted output in constrained boundaries [34]. The GHL law can be written as

$$\Delta w^j(k) = \eta\left[y^j(k)\cdot x^j(k) - y^j(k)\sum_{k=1}^{n} w^j(k) y(k)\right] \tag{31}$$

Using the GHL law defined in (31), the approach can be extended for adaptive droop gains to compensate for the disturbance in finite time. From Fig. 5, the reference value generated for the voltage loop can be written as

$$v_{ref}^j = v_{bus} + \delta v^j - i_o^j\left[R_d^\sigma + r_d^j\right] \tag{32}$$

where, δv^j is the difference between the main bus voltage and terminal voltage of the j^{th} converter, while R_d^σ refers to the adaptive droop gain adjustment as

$$R_d^\sigma = \underbrace{[u_{pi} + u_{hebb}]}_{u_{adap}} e_i^j \tag{33}$$

Considering the difference in branch current as a state vector which directly affects the reference generated for bus voltage; this can be written as

$$e^j = i_o^i - i_o^j \tag{34}$$

To avoid confusion, e^j refers to the j^{th} converter current error and i_o^i, i_o^j denote branch current of i^{th} and j^{th} converter in the microgrid. The general expression for the PI controller to compensate the error can be written as

$$u_{pi} = k_p^j e^j + \int k_i^j e^j \tag{35}$$

where k_p, k_i refers to the PI proportional and integral gains. The generalized Hebb learning based adaptive PI (GHLA-PI) algorithm for the finite time disturbance compensation can be written as [13],

$$u_{adap} = \underbrace{\left[e^j(k)\right]}_{state\,vector} \cdot \underbrace{\left[\hat{\omega}_1(k) + k_p^j\right]}_{cumulative\,weights} + \left[\hat{\omega}_2(k) + \int k_i^j\right] e^j \tag{36}$$

The above equation predominantly illustrates the gains adjustment of PI controller using GHL law for finite time disturbance compensation. Therefore, (33) can be further generalized by using equations (31) and(36) as,

$$R_d^\sigma = \sum_{\mathbf{N}=1\ldots\eta}\left[\Delta w_{\mathbf{N}}^j(k) + k_{pi}^j\right] e^j \tag{37}$$

IV. Performance Evaluation

In efforts to evaluate the performance of the proposed method, a DC microgrid comprising four DGs sharing a common bus is considered. Each DG is interfaced to the common bus with an asynchronous buck converter with 96 VDC as its input and regulating a reference voltage of 48 V at the common bus. The buck converters are rated at 2 kW each, operating at a switching frequency of 10 kHz, a control bandwidth of 2.5 kHz and overall losses limited to 12.3% as per the design criteria. Two types of constant power loads (CPL), critical and noncritical, are connected to the common bus.

The performance is evaluated thoroughly by means of simulations using Matlab/Simulink and its real-world applicability is verified through experimental validation. For a fair comparison, the proposed method is initially evaluated with conventional droop control [5] and dynamic consensus-based distributed three-level droop control (DPID) [35]. To assess the performance of the controllers for finite time disturbance compensation and the viability of controllers to retain asymptotic stability, we further compare the proposed method with droop based SMC proposed in [36]. The system and controller parameters for simulation and experimental evaluation are presented in Table I and II.

A. Simulation Results

Four different cases have been chosen for the performance evaluation of the proposed control: (i) step change in load, (ii) disturbance mitigation, resilience to (iii) DG disconnection, and (iv) communication delays.

*1) **Step Change in Load**:* The response of the proposed method, DPID, and conventional droop to a step change in load from 2 kW to 2.2 kW at 0.05 s, and to 5.5 kW at 0.1 s is shown in Fig. 7. It is important to note that the line impedances for converters connecting the main bus are deliberately varied for the proposed method. In contrast, equal line impedance are considered for both DPID and conventional droop methods. Along with constant line impedance, we also take into account a constant droop coefficient of 0.45 to ensure ΔV in the range of ± 10 V for accommodating fluctuations

TABLE I: System Parameters for Simulation and Experiment

Description	Symbol	Value
Converters Parameters		
Bus Voltage	v_{bus}	$48v$
Load Resistance	$R^{i,j}$	$10\,\Omega$
Control Bandwidth	f_{bw}	2.5 kHz
Switching Frequency	f_{sw}	10 kHz
Inductors, Capacitors	$L^{i,j}$, $C^{i,j}$	200 µH, 230 µF
Input Voltage, Output Voltage	v_{in},v_{out}	$96v$, $48v$
Droop Parameters		
Droop Resistance	R_{droop}	$0.5\,\Omega$
Initial Droop Coefficients	r_d^i, r_d^j	$0.25, 0.45$

TABLE II: Controller Parameters

Notation	Value	Notation	Value
c_1, c_2	2.5, 25	k_i^i	1.5
λ, χ	0.01, 100	k_p^i	0.0025
γ, ζ	0.10, 0.04	k_p^j, k_i^j	22, 0.5
τ	10^{-4}	w_1, w_2	50, 50

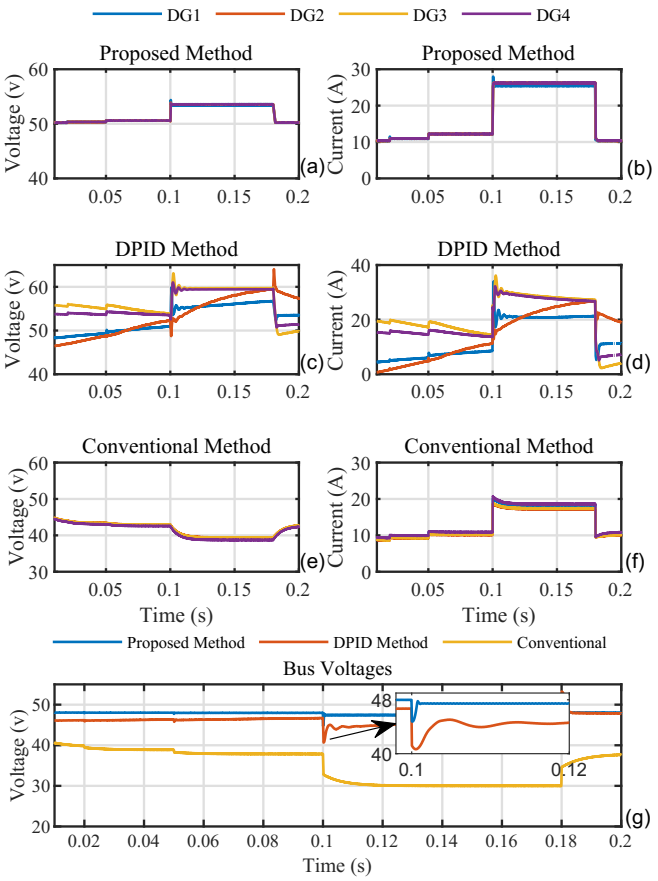

Fig. 7: Response to step change in load, (a) voltage, and (b) current of the proposed method, (c) voltage, and (d) current of the DPID method in [35], (e) voltage, and (f) current of conventional droop method, and (g) comparison of common bus voltage.

in the current. From the illustrations in Fig. 7 (a-b) for load variations, it is evident that the proposed method accurately shares the bus load with fast transitions and provides smooth convergence to the desired voltage and current values. To the contrary, disproportionate sharing of load current and poor bus voltage regulation can be observed in Fig. 7(c, d) for the three-level consensus-based approach and in Fig. 7(e, f) for the conventional droop approach. In terms of common bus voltage regulation, the proposed control exhibits superior performance to DPID and the conventional droop approach even with varying line impedances as shown in Fig. 7g. This shows that the constant droop coefficient does not provide enough flexibility to dynamically change the voltage while accommodating fast variations in the current. Sudden large changes in load demand a rapid response from the controller to mitigate fast transients, else the gains are saturated and stagnant performance is observed. Hence, the proposed method outperforms the consensus-based DPID approach for small and large changes in load, demonstrating resiliency against uncertain conditions challenging the stability of the microgrid.

*2) **Disturbance Mitigation**:* To assess the performance under parametric uncertainty, for finite time disturbance compensation, and viability of controllers to retain asymptotic stability, the proposed method is compared with droop based SMC proposed in [36]. The capacitor and inductor parameters

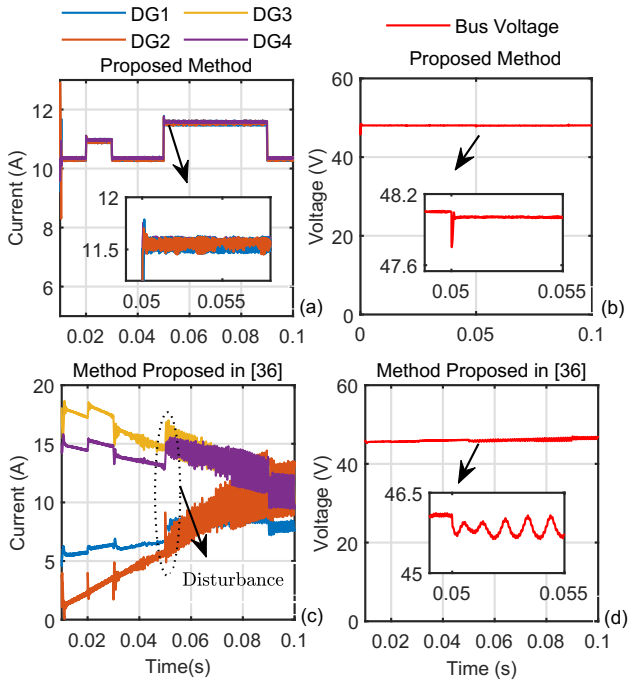

Fig. 8: Response to parametric uncertainty and distrubance injection using the proposed method (a) for DGs current. (b) Bus voltage, and method in [36], (c) for DGs current (d) Bus voltage.

of the converter are chosen to be within 15% of the nominal values presented in Table I. The initial line resistances for DG1, DG2, DG3 and DG4 are $0.5\,\Omega$, $0.4\,\Omega$, $0.8\,\Omega$ and $0.75\,\Omega$ respectively and are varied up to 10% their nominal values at 25 ms. Furthermore, an external disturbance of $d_v(t) = d_v \sin(15t)$ is added at 50ms. It can be observed from Fig. 8 that the method proposed in [36] takes a long time to converge with considerable oscillations in the DGs current. This precisely occurs due to control loop instability and results in excess voltage oscillations that specifically start at 50ms when an external disturbance is injected into the system. In terms of bus voltage regulation, the method proposed in [36] exhibits sustained oscillations, as shown in Fig. 8(d). On the other hand, the proposed method ensures proportional current sharing demonstrating robust disturbance rejection capability. Furthermore, the bus voltage experiences a dip of 0.2 V stabilizing at 48 V. The efficacy of the proposed method is due to the characteristics of the generalized Hebb rule where the weights of the control loop adjust the droop gains in finite time for any disturbance in the system. This enables the control loop in bounded limits to mitigate the disturbance and minimize the error in finite time.

*3) **DG Outage**:* The third case evaluates the performance of the proposed method when a DG is disconnected. The DGs have the same rated power and unequal line resistance i.e., $0.5\,\Omega$, $0.25\,\Omega$, $0.8\,\Omega$ and $0.4\,\Omega$ for DG1, DG2, DG3 and DG4, respectively. The performance of the proposed control to loss of DG at 10 ms is presented in Fig. 9. The current reference of all the DGs adjusts to a new set point soon after 10 ms, resulting in equal sharing of load current without any overshoots and oscillations in current. This further demonstrates the efficacy of the proposed controller in adjusting the gains in finite time to respond robustly to the disconnection of a DG.

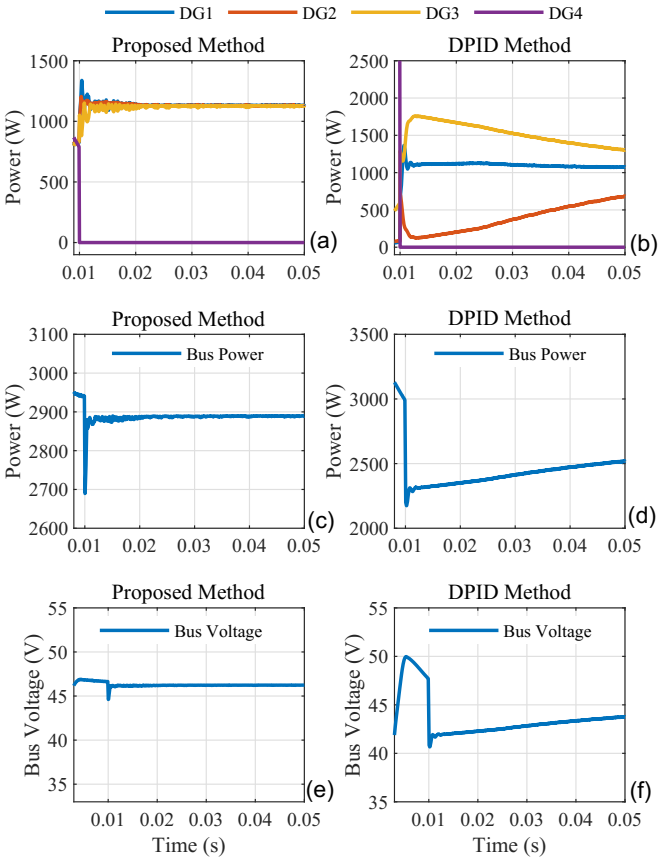

Fig. 9: Effect of DGs disconnection and communication failure on load bus: DGs current using, (a) proposed method, (b) DPID in [35], load bus power using (c) proposed method, (d) DPID in [35], and load bus voltage using (e) proposed method, (f) DPID in [35].

On the contrary, the DPID-based approach has undesirable performance, as shown in Fig. 9(b, d and f), where DG2 and DG3 outputs present a large deviation from their reference.

*4) **Communications Delay**:* In this section, the robustness of the proposed approach under presence of delays is evaluated. The average delays within Great Britain are presented in Table III. Considering the distances for the evaluated delays, it can be concluded that the delays within a microgrid will be much lower. However, the performance of the proposed control by incorporating a 10 ms delay is shown in Fig. 10. It can be observed that the 10 ms communication delay has minimal impact on both the DG output current and load bus voltage when compared to the system without delay. It can therefore be concluded that the proposed method accommodates the maximum communication delay in finite time, regulates the DG output current, and maintains constant load bus voltage effectively.

B. Experimental Validation

The proposed approach is validated experimentally at the Indian Institute of Technology, Bhubhaneswar. The experimental setup, as shown in Fig. 11, comprises of battery energy storage system (BESS) and photovoltaic (PV) emulator at 96 VDC interfaced to a common bus via asynchronous buck

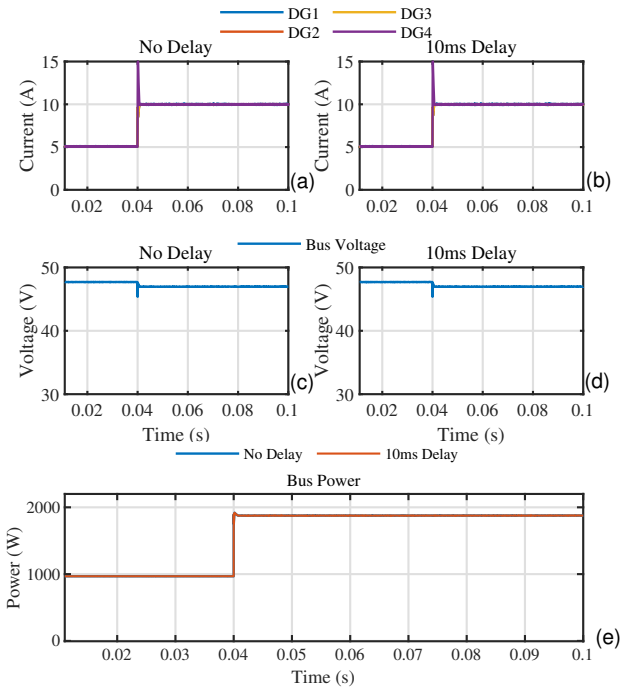

Fig. 10: Performance of the proposed method under communications delays: DGs current under (a) no delay, (b) 10 ms delay, load bus voltage under (c) no delay, (d) 10 ms delay, and (e) the load bus power.

TABLE III: Average time delays within Great Britain [37]

	Cardiff	Coventry	Manchester	Newcastle
London	5.577 ms	5.915 ms	6.073 ms	9.49 ms

converters rated at 1 kW each. The converters are coupled to the main bus via lines of unequal resistances while the load is directly connected to the main bus. The proposed control has been synthesized on a TI F28379D microprocessor offering analog to digital and digital to analog conversation at 12 bits resolution with a 2 MHZ clock frequency. Two test cases, (i) DGs disconnection and restoration and (ii) step change in load are performed to briefly illustrate the performance of the proposed controller in prototypical conditions.

1) DG Disconnection and Restoration: The DC bus voltage is regulated at 48V DC when two DGs (Buck Converters) are feeding a CPL through a common bus and sharing a proportionate current for a load of 480 W as shown in Fig. 12a. A 10 % parametric uncertainty is incorporated compared to the nominal values in Table I for converters. As can be observed, the proposed control effectively regulates the bus voltage with DG1 increasing its power output to compensate for the loss of DG2. Fig. 12b presents the performance of the proposed control when the disconnected DG is restored. The performance of the controller is evident for regulating bus voltage, ensuring proportionate sharing of load current and providing minimal transient condition on DC bus after DG restoration.

2) Step Change in Load: The performance of the controller for step change in load is demonstrated in Fig.12c and Fig.12d while considering the same conditions as in the previous case. An additional 50 % (240 W) programmable load is switched in

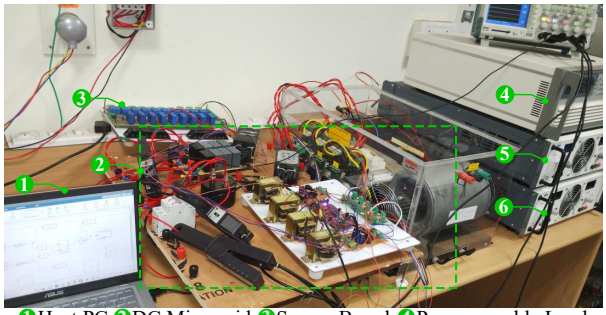

(a) Hardware Configuration

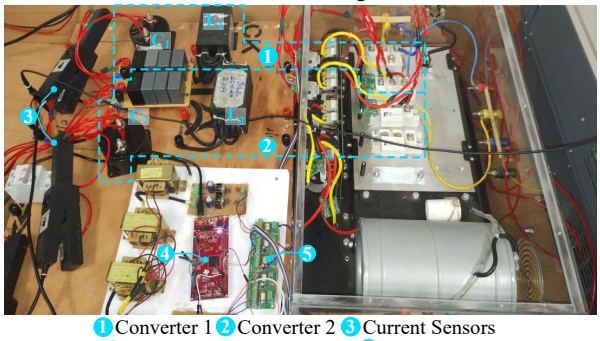

(b) Zoomed in DC Microgrid

Fig. 11: Experimental Setup

at 140 ms. The desired tracking of constant DC bus voltage and proportionate sharing of current is ensured by compensating the droop gains using GHL in finite time as demonstrated in Fig.12c. Similarly, Fig.12d validates the efficacy of the proposed approach for stabled DC bus voltage while deactivating step load of 50% on the DC bus. It is evident that the controller adapts the gains in finite time for both conditions and stabilizes the load bus with 48V while resulting in only a 2% error in proportionate sharing of current for both converters.

V. Conclusions

The parallel operation of power converters in DC microgrids by droop control exhibits a trade-off between voltage and current due to constant and linear droop coefficients. The performance of the control method deteriorates when varying the loading conditions and disturbance parameters affect the droop coefficients. Therefore, an alternate approach that can adjust the droop gains in finite time for disturbance compensation and load variation is required to ensure the stability and regulated power. This work proposes hybrid droop control using fractional order sliding mode and generalized Hebbian learning algorithm for DC microgrids. The approach mitigates the effect of disturbances and preserves the constant reference for the secondary loop to maintain a desired bus voltage. The performance of the proposed method is evaluated for step loads, varying parameters that affect the droop coefficients, DG outage and full load conditions. The comparative analysis shows the effectiveness of this method for DC microgrid applications requiring constant bus voltage and tight margins for proportionate load power sharing. The rapid control prototyping, validation using Matlab/Simulink and hardware

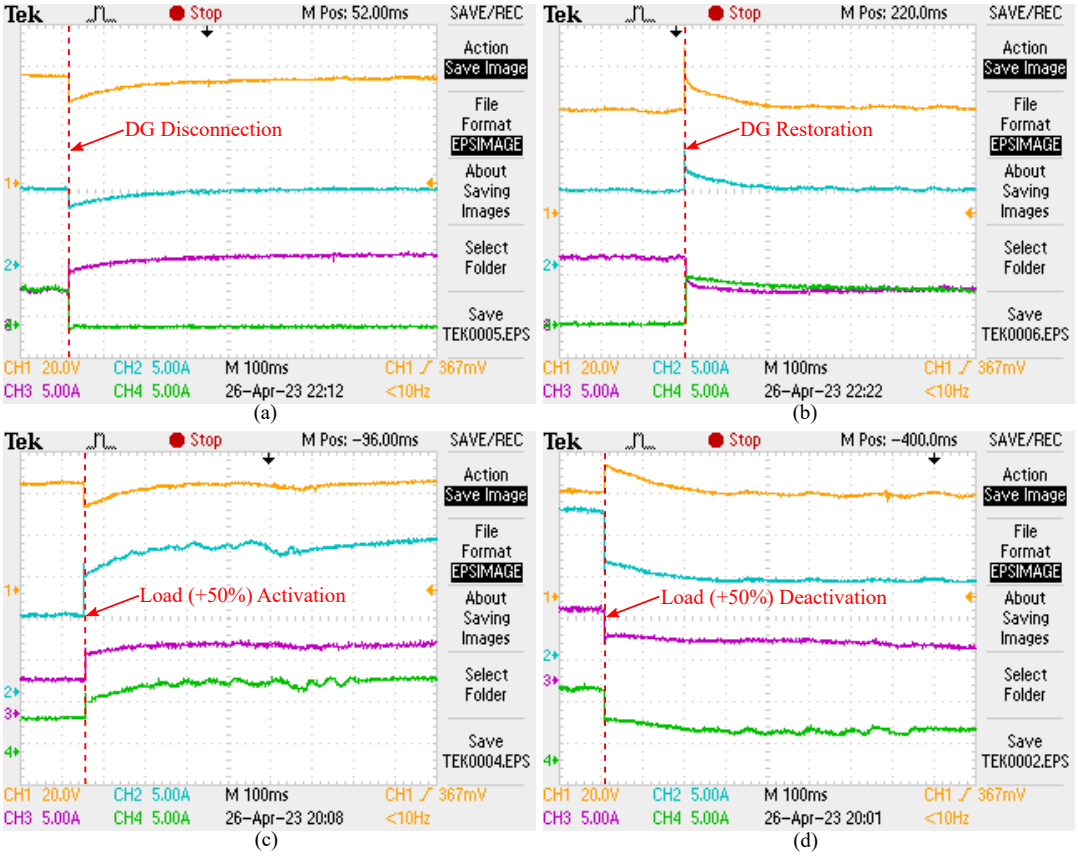

Fig. 12: Experimental results for (a) DGs disconnection, (b) DGs restoration, (c) step load activation, (d) step load deactivation. Legend: CH1: Main bus voltage, CH2: Main bus current, CH3: DG1 output current, CH4: DG2 output current.

experiment demonstrate the efficacy of the proposed method for resilient DC microgrids. Future work will explore the application of the proposed approach to wider power and energy networks, supporting the scalability and enhancing the resilience of the whole system.

REFERENCES

[1] R. Lasseter, A. Akhil, C. Marnay, and J. Stevens, "The certs microgrid concept - white paper on the integration of distributed energy resources," 2002, technical report, U.S. Department of Energy.

[2] D. Park and M. Zadeh, "Modeling and predictive control of shipboard hybrid dc power systems," *IEEE Trans. Transp. Electrification*, vol. 7, no. 2, pp. 892–904, 2021.

[3] T. Dragičević, X. Lu, J. C. Vasquez, and J. M. Guerrero, "Dc microgrids—part i: A review of control strategies and stabilization techniques," *IEEE Trans. Power Electron.*, vol. 31, no. 7, pp. 4876–4891, 2016.

[4] J. Hou, Z. Song, H. F. Hofmann, and J. Sun, "Control strategy for battery/flywheel hybrid energy storage in electric shipboard microgrids," *IEEE Trans. Ind. Informat.*, vol. 17, no. 2, pp. 1089–1099, 2021.

[5] Y. Lin and W. Xiao, "Novel piecewise linear formation of droop strategy for dc microgrid," *IEEE Trans. Smart Grid*, vol. 10, no. 6, pp. 6747–6755, 2019.

[6] F. Chen, R. Burgos, D. Boroyevich, J. C. Vasquez, and J. M. Guerrero, "Investigation of nonlinear droop control in dc power distribution systems: Load sharing, voltage regulation, efficiency, and stability," *IEEE Trans. Power Electron.*, vol. 34, no. 10, pp. 9404–9421, 2019.

[7] Z. Jin, L. Meng, J. M. Guerrero, and R. Han, "Hierarchical control design for a shipboard power system with dc distribution and energy storage aboard future more-electric ships," *IEEE Trans. Ind. Informat*, vol. 14, no. 2, pp. 703–714, 2018.

[8] B. Li, Q. Li, Y. Wang, W. Wen, B. Li, and L. Xu, "A novel method to determine droop coefficients of dc voltage control for vsc-mtdc system," *IEEE Trans. Power Del.*, vol. 35, no. 5, pp. 2196–2211, 2020.

[9] Sandeep Anand and Baylon G. Fernandes and Josep M. Guerrero, "Distributed Control to Ensure Proportional Load Sharing and Improve Voltage Regulation in Low-Voltage DC Microgrids," *IEEE Trans. Power Electron.*, vol. 28, no. 4, pp. 1900–1913, 2013.

[10] Sahoo, Saroja Kanti and Sinha, Avinash Kumar and Kishore, N. K., "Control Techniques in AC, DC, and Hybrid AC–DC Microgrid: A Review," *IEEE Journal of Emerging and Selected Topics in Power Electronics*, vol. 6, no. 2, pp. 738–759, 2018.

[11] Q.-C. Zhong, "Robust droop controller for accurate proportional load sharing among inverters operated in parallel," *IEEE Trans. Ind. Electron.*, vol. 60, no. 4, pp. 1281–1290, 2013.

[12] Hamidieh, Mohammad and Ghassemi, Mona, "Microgrids and Resilience: A Review," *IEEE Access*, vol. 10, pp. 106 059–106 080, 2022.

[13] Li, Yilin and Dong, Ping and Liu, Mingbo and Yang, Guokang, "A Distributed Coordination Control Based on Finite-Time Consensus Algorithm for a Cluster of DC Microgrids," *IEEE Trans. Power Syst.*, vol. 34, no. 3, pp. 2205–2215, 2019.

[14] Xing, Lantao and Mishra, Yateendra and Guo, Fanghong and Lin, Pengfeng and Yang, Yang and Ledwich, Gerard and Tian, Yu-Chu, "Distributed Secondary Control for Current Sharing and Voltage Restoration in DC Microgrid," *IEEE Trans. Smart Grid*, vol. 11, no. 3, pp. 2487–2497, 2020.

[15] Sahoo, Subham and Mishra, Sukumar, "A Distributed Finite-Time Secondary Average Voltage Regulation and Current Sharing Controller for DC Microgrids," *IEEE Trans. Smart Grid*, vol. 10, no. 1, pp. 282–292, 2019.

[16] Wang, Panbao and Huang, Rui and Zaery, Mohamed and Wang, Wei and Xu, Dianguo, "A Fully Distributed Fixed-Time Secondary Controller for DC Microgrids," *IEEE Trans. Ind. Appl.*, vol. 56, no. 6, pp. 6586–6597, 2020.

[17] Malek, Sajjad and Gholipour, Mehdi, "Robust scheme for voltage regulation and power sharing among DERs in DC microgrids," *IET Renewable Power Generation*, vol. 14, no. 4, pp. 647–657.

[18] S. Sahoo *et al.*, "A cooperative adaptive droop based energy management and optimal voltage regulation scheme for dc microgrids," *IEEE Trans. Ind. Electron.*, vol. 67, no. 4, pp. 2894–2904, 2020.

[19] F. Chen, R. Burgos, D. Boroyevich, J. C. Vasquez, and J. M. Guerrero, "Investigation of nonlinear droop control in dc power distribution systems: Load sharing, voltage regulation, efficiency, and stability," *IEEE Trans. Power Electron.*, vol. 34, no. 10, pp. 9404–9421, 2019.

[20] P. Prabhakaran, Y. Goyal, and V. Agarwal, "Novel nonlinear droop control techniques to overcome the load sharing and voltage regulation issues in dc microgrid," *IEEE Trans. Power Electron.*, vol. 33, no. 5, pp. 4477–4487, 2018.

[21] Y. Zhang, X. Qu, M. Tang, R. Yao, and W. Chen, "Design of nonlinear droop control in dc microgrid for desired voltage regulation and current sharing accuracy," *IEEE Journal on Emerging and Selected Topics in Circuits and Systems*, vol. 11, no. 1, pp. 168–175, 2021.

[22] H. M. Soliman, E. H. E. Bayoumi, F. A. El-Sheikhi, and A. M. Ibrahim, "Ellipsoidal-set design of the decentralized plug and play control for direct current microgrids," *IEEE Access*, vol. 9, pp. 96 898–96 911, 2021.

[23] Y. Mi *et al.*, "Intelligent power sharing of dc isolated microgrid based on fuzzy sliding mode droop control," *IEEE Trans. Smart Grid*, vol. 10, no. 3, pp. 2396–2406, 2019.

[24] Y. Li *et al.*, "An adaptive droop control scheme based on sliding mode control for parallel buck converters in low-voltage dc microgrids," in *2021 IEEE 4th International Electrical and Energy Conference (CIEEC)*, 2021, pp. 1–6.

[25] A. Cristiane Buzzi *et al.*, "Sliding mode based droop control strategies for parallel-connected inverters in railway vehicles," in *2020 European Control Conference (ECC)*, 2020, pp. 1891–1896.

[26] M. R. D. Hebb, "The organization of behavior," Wiley, pp. 5–6, 1949.

[27] Z. Wang, S. Li, and Q. Li, "Continuous nonsingular terminal sliding mode control of dc–dc boost converters subject to time-varying disturbances," *IEEE Trans. Circuits Syst. II, Exp. Brief*, vol. 67, no. 11, pp. 2552–2556, 2020.

[28] M. Mosayebi *et al.*, "Intelligent and fast model-free sliding mode control for shipboard dc microgrids," *EEE Trans. Transp. Electrification*, vol. 7, no. 3, pp. 1662–1671, 2021.

[29] X. Lin *et al.*, "Fractional-order sliding mode approach of buck converters with mismatched disturbances," *IEEE Trans. Circuits and Systems I: Regular Papers*, vol. 68, no. 9, pp. 3890–3900, 2021.

[30] J. Yang, S. Li, and X. Yu, "Sliding-mode control for systems with mismatched uncertainties via a disturbance observer," *IEEE Trans. Ind. Electron.*, vol. 60, no. 1, pp. 160–169, 2013.

[31] Z. Farooq *et al.*, "Artificial neural network based adaptive control of single phase dual active bridge with finite time disturbance compensation," *IEEE Access*, vol. 7, pp. 112 229–112 239, 2019.

[32] M. Nasir, Z. Jin, H. A. Khan, N. A. Zaffar, J. C. Vasquez, and J. M. Guerrero, "A decentralized control architecture applied to dc nanogrid clusters for rural electrification in developing regions," *IEEE Trans. Power Electron.*, vol. 34, no. 2, pp. 1773–1785, 2019.

[33] C. Napole, O. Barambones, I. Calvo, and J. Velasco, "Feedforward compensation analysis of piezoelectric actuators using artificial neural networks with conventional pid controller and single-neuron pid based on hebb learning rules," *Energies*, vol. 13, no. 15, 2020.

[34] K. Joutsensalo, "A nonlinear extension of the generalized hebbian learning," *Neural Processing Letters*, vol. 2, pp. 5–8, 1995.

[35] H. Wang *et al.*, "Distributed secondary and tertiary controls for i-v droop-controlled paralleled dc-dc converters," *IET Generation, Transmission and Distribution*, vol. 12, no. 7, pp. 2894–2904, 2018.

[36] M. Veysi *et al.*, " Robust, Accurate, and Fast Decentralized Power Sharing Mechanism for Isolated DC Microgrid Using Droop-Based Sliding-Mode Control," *IEEE Trans. Smart Grid*, vol. 13, no. 6, pp. 4160–4173, 2022.

[37] Global ping statistics. [Online]. Available: https://wondernetwork.com/pings

Taimur Zaman recieved his B.Sc degree in electrical power from COMSATS University, Islamabad, Pakistan in 2015 and M.Sc degree in power and control engineering from CECOS University, Peshawar, Pakistan, in 2019. He is pursuing Ph.D in electronics and electrical engineering at the University of Strathclyde, Glasgow, UK. His research area is focused on power system disturbance identification, resiliency & control. Before he started his PhD in June 2021, he worked as R&D engineer facilitating development projects related to power systems and control. He has also been working as a research assistant at CECOS University of Science and Technology, Pakistan, from 2017-2019.

Zhiwang Feng (Member, IEEE) received the B.Eng., M.Sc., and Ph.D. degrees in electronic and electrical engineering from the North China Electric Power University, the University of Manchester, and the University of Strathclyde, in 2017, 2018, and 2023 respectively. He works as a research associate, leading the microgrid and power hardware-in-the-loop experimental validation at the Dynamic Power Systems Laboratory within the Institute for Energy and Environment at the University of Strathclyde. His research interests include geographically distributed real-time simulation, real-time power hardware-in-the-loop simulation, and their applications to the experimental validation of power converters, microgrid control, and electric power systems.

Sanjib Mitra (Student Member, IEEE) was born in Kolkata, India. He received the B.Tech. degree in electrical engineering from the Calcutta Institute of Engineering and Management, Kolkata, India, in 2010 and the M.Tech. degree in electrical engineering from the University of Calcutta, Kolkata, India, in 2012. He is currently pursuing the Ph.D. degree in electrical engineering with the Indian Institute of Technology Bhubaneswar, Bhubaneswar, India.

His current research interests include high-gain DC-DC converters, renewable energy integration, hybrid energy storage integration and advanced energy management system.

Mazheruddin Syed (Member, IEEE) received the B.E. degree in electrical and electronics engineering from Osmania University, Hyderabad, India, in 2011, the M.Sc. degree in electrical power engineering from the Masdar Institute of Science and Technology, Abu Dhabi, UAE, in 2013, and the Ph.D. degree in electrical power systems from the University of Strathclyde, Glasgow, Scotland, in 2018.,He is currently the Power Systems Lead for Scotland at WSP, U.K., working on innovation projects with transmission and distribution system operators. Before joining WSP, he was a Strathclyde Chancellor's Fellow (Lecturer/Assistant Professor) with the Department for Electronic and Electrical Engineering, University of Strathclyde, Glasgow, and was the Manager of the Dynamic Power Systems Laboratory. Prior to his position as a Chancellor's Fellow, he was a Research Fellow with the Institute for Energy and Environment, University of Strathclyde. He has contributed to innovative power system research projects with a strong publication record of more than 70 peer-reviewed papers in top-tier journals and conferences. His research interests include decentralized and distributed control, real-time controller and power hardware in the loop simulations, and systems level validations.,Dr. Syed is active in a number of national and international committees. He is the Technical Committee Secretary of IEEE PES Task Force on Cloud-Based Control and Co-Simulation of Multi-Party Resources.

Srinivas Karanki (Senior Member, IEEE) was born in Visakhapatnam, India. He received the B.Tech. degree from the Acharya Nagarjuna University, Guntur, India, in 2007 and the Ph.D. degree in electrical engineering from the Indian Institute of Technology Madras, Chennai, India, in 2012.

From 2012 to 2014, he was a Postdoctoral Fellow with the Centre for Urban Energy, Ryerson University, Toronto, ON, Canada. He is currently an Associate Professor with the School of Electrical Sciences, Indian Institute of Technology Bhubaneswar, Bhubaneswar, India. His current research interests include power electronic converters for renewable energy systems, power quality, energy storage, and power electronics applications in power systems.

Luiz Villa (Member, IEEE) graduated from electrical engineering from the University of Santa Catarina, Brazil in 2009. He obtained his PhD in electrical engineering at the University of Grenoble in 2013 and has been an associate professor at the University of Toulouse since 2014. His work focuses on software defined and data driven power electronics. His objective is to create power electronics converters that are multi-purpose, reprogrammable, with multiple lifetimes and open-source. To do so, he has worked on using the data from the power converter itself for offline diagnosis through machine learning techniques.

Graeme M. Burt (M'95) received the B.Eng. degree in electrical and electronic engineering and the Ph.D. degree in fault diagnostics in power system networks from the University of Strathclyde, Glasgow, U.K., in 1988 and 1992, respectively. He is currently a Distinguished Professor of electrical power systems with the University of Strathclyde where he directs the Institute for Energy and Environment, directs the Rolls-Royce University Technology Centre in Electrical Power Systems, and is Lead Academic for the Power Networks Demonstration Centre (PNDC). In addition, he serves on the board of DERlab e.V., the association of distributed energy laboratories. His research interests include the areas of decentralized energy and smart grid protection and control, electrification of aerospace and marine propulsion, dc and hybrid power distribution, and experimental systems testing and validation with power hardware in the loop.